**Journal of Mechanical, Civil and Industrial Engineering**
ISSN: 2709-0809
DOI: 10.32996/jmcie
Journal Homepage: www.al-kindipublisher.com/index.php/jmcie

# Improving Air Filtration Based on PM2.5 Distribution

**Nguyen An Gia Huy**[1], **Hoang Thi Hong Minh** ✉[2]

[1] *Hanoi Amsterdam High School for Gifted Students*

[2] *MKAC Meiko Automation*

**Corresponding Author:** Hoang Thi Hong Minh**, E-mail:** hoanghongminh13@gmail.com

## ABSTRACT

Dust concentrations in enclosed environments often exhibit considerable spatial variability, meaning that measurements taken at a single location may fail to capture localized areas of elevated exposure. To address this limitation, this study develops a spatial mapping approach for characterizing PM2.5 concentrations in a controlled test room and evaluating the influence of air filter placement on indoor particle distribution. A portable monitoring device integrating an ESP32 microcontroller and a PMS5003 particulate matter sensor is employed to collect measurements from 16 predefined sampling locations, with data automatically transmitted to Google Sheets. At each sampling point, a 30-second stabilization period is implemented before data collection, and consecutive valid readings are averaged to obtain representative PM2.5 concentrations. Spatial concentration distributions are subsequently reconstructed using Python-based inverse distance weighting (IDW) interpolation to visualize pollution patterns and identify potential exposure hotspots. The performance of different filter placement configurations is assessed through multiple quantitative indicators, including mean and maximum PM2.5 concentrations, hotspot frequency, and integrated pollutant concentration across identified hotspot areas. Comparative results and the optimal filter configuration will be established upon completion of the experimental measurements. Overall, this study proposes a preliminary, data-driven framework for spatially evaluating particulate matter distribution and optimizing air filter positioning. Further experimental validation under representative industrial conditions is necessary before extending the proposed approach to practical workshop environments.

## KEYWORDS

PM2.5, Indoor air filtration, Low-cost air quality monitoring, Spatial interpolation, Inverse distance weighting

## ARTICLE INFORMATION

**ACCEPTED:** 11 October 2026 **PUBLISHED:** 11 November 2026 **DOI:** 10.32996/jmcie.2026.7.6.5

## 1. INTRODUCTION

PM2.5 dust in production environments—generated by processes such as material machining, cutting, and grinding—is often unevenly distributed due to factors like distance from the source, airflow direction, obstacles, and the specific ventilation setup. Consequently, relying on data from a single fixed sensor or a room-wide average can overlook localized areas of high concentration.

Optical sensing technology enables the construction of portable PM2.5 monitoring devices Invalid source specified., Invalid source specified.. In this study, an ESP32 microcontroller reads data from a PMS5003 sensor via UART and transmits it to a Google Sheet over Wi-Fi. To ensure data validity, the program verifies the data frame structure and checksum before recording the readings. However, optical sensor results can still be influenced by humidity and specific types of dust particles Invalid source specified., Invalid source specified..

Previous studies have shown that multi-location measurements help identify spatial variations in PM2.5 concentrations Invalid source specified.. Air purifier effectiveness is also commonly assessed by comparing concentration levels before and after operation Invalid source specified.. Building on this, the present study evaluates the suitability of the monitoring device by generating PM2.5 distribution maps to analyze the impact of purifier placement during laboratory testing. The study focuses on the following aspects: constructing the monitoring device; conducting sequential measurements with a single device across three different test scenarios; generating PM2.5 maps using the Inverse Distance Weighting (IDW) interpolation method Invalid source specified. based on the room's actual layout; and comparing purifier placement options using both statistical and spatial data.

**Copyright:** © 2026 the Author(s). This article is an open access article distributed under the terms and conditions of the Creative Commons Attribution (CC-BY) 4.0 license (https://creativecommons.org/licenses/by/4.0/). Published by Al-Kindi Centre for Research and Development, London, United Kingdom.

While the results assist in selecting purifier locations for the tested conditions, they do not provide a sufficient basis to determine a universally optimal location for all environments.

The recent literature shows two related but separate lines of work. The first line evaluates low-cost PM sensors through co-location, calibration and environmental correction. The second line evaluates portable air cleaners in homes, classrooms or offices. These studies show that low-cost sensors can support spatial screening, but their readings should be interpreted together with calibration information and the conditions under which the measurements were collected [7], [8], [9], [10], [11]. They also show that the effect of a portable air cleaner depends on room size, background concentration, operating time, ventilation and the position of the cleaner [5], [12], [13], [14], [15].

A smaller number of studies directly combine a low-cost sensor, a room-scale concentration map and a comparison of purifier locations. This study addresses that practical gap by using one portable ESP32-PMS5003 device to measure 16 points in the same room under three scenarios. The aim is not to establish a universal purifier location or to replace a reference monitor. Instead, the aim is to determine whether a simple measurement and IDW mapping procedure can identify the higher-concentration area and distinguish the two tested purifier positions under the conditions of this experiment.

## 2. METHOD

### *2.1 Measurement system*

The ESP32-WROOM-32D reads the PMS5003 particulate sensor over UART2 at 9600 baud/s and uploads recorded values to Google Sheets via Wi-Fi. A two-cell lithium-ion battery pack powers the suspended measurement unit. A Xiaomi Smart Air Purifier 4 Compact provides the filtration intervention. The sensor protocol and module characteristics follow the manufacturers' technical documentation [16], [17].

Table 1: Experimental Hardware

| Component | Model | Function |
|---|---|---|
| Microcontroller | ESP32-WROOM-32D | UART acquisition and aggregation |
| Particle sensor | PMS5003 | PM2.5 reading |
| Air purifier | Xiaomi Smart Air Purifier 4 Compact | Filtration in S1 and S2 |
| Power supply | Two lithium-ion cells | Portable measurement supply |

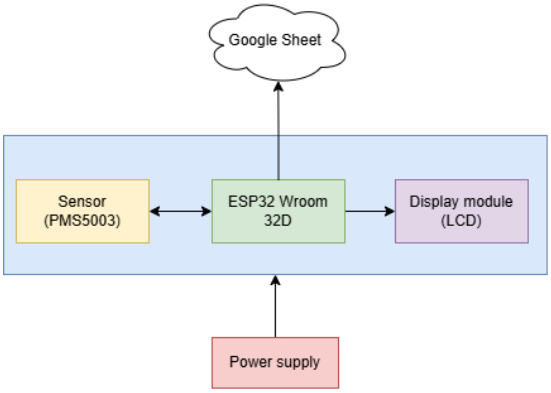



Figure 1. System block diagram

### *2.2 Measurement quality assurance and validity*

The measurement protocol included checks for both data transmission and short-term reading stability. At the firmware level, a reading was accepted only when the PMS5003 frame header, packet length and checksum were valid. This rule removes incomplete or corrupted UART packets from the dataset. It does not prove that the reported concentration is accurate. In this study, frame validation is therefore treated as an internal data-quality check, not as calibration against a reference instrument.

At each sampling point, a 30-second stabilization period was applied before data collection. Thirty valid frames were then retained and divided into three consecutive blocks of ten frames. The block means R1, R2 and R3 were recorded separately before the point estimate was calculated. This structure provides a simple within-visit repeatability check: the spread among R1, R2 and R3 can reveal short-term instability, transient airflow, or movement of the operator. Because the blocks were collected consecutively, they are not independent replicates and were not treated as independent observations in the scenario comparison.

The same sensor, firmware, battery arrangement and measurement locations were used in S0, S1 and S2. This makes the comparison more consistent because the three scenarios were measured with the same equipment. However, the design does not control changes in door and window state, fan operation, human activity, source emission rate or outdoor PM2.5. These factors were not logged during the experiment. The results therefore describe the tested measurement sequence; they do not provide a causal estimate of the effect of purifier placement.

### *2.3 Data processing and reproducibility*

For each point i, the representative concentration was calculated as $C_i = \frac{R_1+R_2+R_3}{3}$. The mean, median, minimum, maximum and spatial standard deviation were then calculated from the 16 point estimates within each scenario. Relative reduction was calculated as $\frac{100(C_a-C_b)}{C_a}$, where $C_a$ is the value in the earlier comparison scenario and $C_b$ is the value in the later scenario. The same 75 $\mu g/m^3$ threshold was applied to all scenarios so that the number of measured hotspots and the IDW exceedance area were comparable.

IDW was selected because some measurement points had to be shifted around benches and other obstructions, while a continuous map was needed to show the room-scale pattern. The exponent was fixed at p = 2 for all scenarios, and interpolation was limited to the room boundary. The map should be treated as a spatial visualization based on the sampling points, not as a model of particle movement. It does not include airflow direction, purifier CADR, particle deposition, resuspension or changes in particle generation and removal. The point coordinates and raw block means should be provided as supplementary data so that the maps and summary statistics can be reproduced.

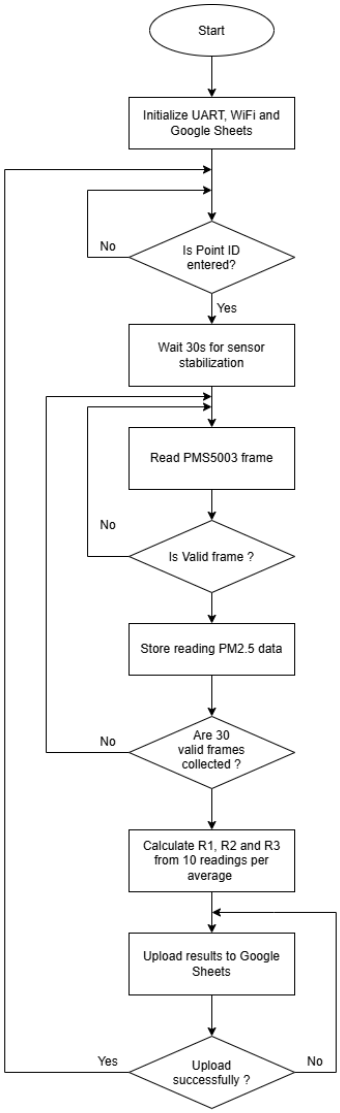



Figure 2. Firmware flowchart

### *2.4 Room and experimental configurations*

The experiment was conducted in a rectangular room measuring 5 × 3.5 m. The coordinate origin was set at the lower-left corner of the room plan. The entrance, windows, fan, laboratory benches, and major obstructions were marked on the plan according to their measured positions.

Sixteen measurement points were arranged on an approximately uniform grid within the accessible area, at a height of about 1.5 m above the floor. Where necessary, points were shifted to remain inside the room or avoid obstructions. The final coordinates of all measurement points should be reported in the supplementary data.



Figure 3. Actual laboratory test room

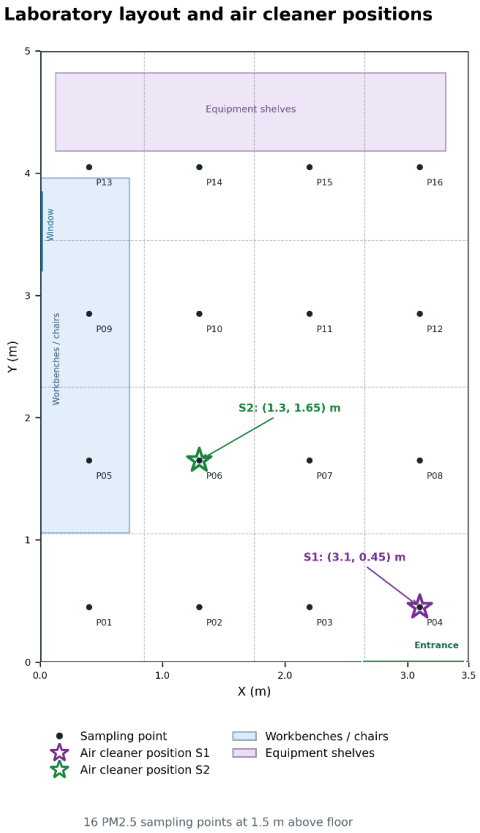



Figure 4. Floor plan and experimental diagram

The study examines three scenarios using the same filtration unit and set of measurement points. In scenario S0, the filter is turned off to record the background PM2.5 distribution. In S1, the filter operates at the initial location (3.10; 0.45) m. In S2, the filter is relocated to a position near the high-concentration area (1.30; 1.65) m. These coordinates are defined based on the room's floor plan layout.

Table 2. Experimental Scenarios

| Scenario | Purifier | Placement |
|---|---|---|
| S0 | Off | Baseline |
| S1 | On | Initial position (3.1, 0.45 m) |
| S2 | On | Relocated position (1.3, 1.65 m) |

The same instrument and location list were used across scenarios. Measurements were made sequentially; contemporaneous changes in activity, doors, ventilation and source emissions were not independently controlled or recorded in the supplied manuscript.

### 2.5 Spatial interpolation and evaluation metrics

The representative PM2.5 value at each measurement point is used to generate a concentration distribution map using the Inverse Distance Weighting (IDW) interpolation method. Interpolation is performed only within the confines of the room. With an exponent of p=2, the concentration at location (x, y) is estimated as follows:

$$\hat{C}(x,y) = \frac{\sum_{i=1}^{n} d_i(x,y)_i^{-p}\overline{C}_i}{\sum_{i=1}^{n} d_i(x,y)^{-p}}, \quad p = 2 \qquad (1)$$

Here, $\overline{C}_i$ represents the value at measurement point $i$, while $d_i(x,y)$ is the distance from that point to the location where interpolation is being performed. If $(x,y)$ coincides with a measurement point, the measured value at that point is used directly.

To compare the scenarios, the study examines the average concentration ($C_{\text{avg}}$), the maximum concentration $C_{max}$, the number of measurement points with PM2.5 levels of 75 $\mu g/m^3$ or higher, and the area exceeding this threshold on the interpolation map. The 75 $\mu g/m^3$ threshold is used to identify hotspots and facilitate comparisons between scenarios in this study.

### 2.6 Experimental sequence and data handling

The three scenarios used the same sensor, the same nominal measurement points and the same room layout. S0 was measured with the purifier switched off, followed by S1 at the initial position and S2 after relocation. Because the measurements were collected sequentially, the scenario order is part of the experimental design and is reported explicitly. The comparison is therefore treated as a descriptive within-room comparison. It is not treated as a randomized experiment, because the order was not randomized and the duration between scenarios was not recorded in the supplied dataset.

For each point, invalid frames were discarded before the three groups of ten valid frames were formed. The point value was then calculated from the three block means rather than from a single instantaneous reading. The same calculation was applied to every point and every scenario. No additional correction for relative humidity or particle composition was applied because temperature and relative humidity were not recorded and the PMS5003 was not co-located with a reference instrument. This choice keeps the reported values close to the sensor output and avoids presenting an unverified correction as a calibrated concentration.

The present data allow comparison of the spatial pattern and the relative change between scenarios. They do not allow an estimate of measurement accuracy, a confidence interval based on independent repeats, or a causal estimate of purifier effectiveness. These limits are important when the results are compared with recent calibration studies, which generally use reference instruments and environmental variables to evaluate sensor performance [18], [19], [20], [21], [22], [23]. Related work has also used low-cost nitrogen dioxide sensors for epidemiologic exposure assessment [24]; those results concern a different pollutant and do not validate the PM2.5 measurements in this study.

## 3. RESULTS AND DISCUSSION

### 3.1 Spatial concentration and purifier placement

In scenario S0, the average PM2.5 concentration across the 16 points was 56.73 $\mu g/m^3$; the minimum, median, and maximum values were 29.90, 58.37, and 91.63 $\mu g/m^3$, respectively. The maximum value occurred at point P09 (0.40; 2.85 m). Two points—P05 and P09, both located in the workstation area—exceeded the 75 µg/m³ hotspot threshold.

The storage table area at the far end of the room (points P13–P16) exhibited concentrations ranging from 54.83 to 63.80 $\mu g/m^3$. Although these values were lower than those at the workstation hotspots, they still formed a zone of relatively high concentration on the interpolated map. The area exceeding the 75 $\mu g/m^3$ threshold, as estimated from the S0 IDW map, was 1.190 $m^2$.

With the purifier at its initial position (S1), the mean reached 52.35 $\mu g/m^3$, a 7.71% decrease relative to S0. The maximum was 84.10 $\mu g/m^3$, and P05 and P09 remained above the threshold. In S2, the mean reached 42.43 $\mu g/m^3$ and the maximum reached 68.07 $\mu g/m^3$; none of the measured locations exceeded the threshold. Relative to S1, these two concentration metrics decreased by 18.94% and 19.06%, respectively.

Table 3. PM2.5 Metrics by Scenario

| Metric | S0 | S1 | S2 |
|---|---|---|---|
| Number of points | 16 | 16 | 16 |
| Minimum (µg/m³) | 29.90 | 26.30 | 24.10 |
| Median (µg/m³) | 58.37 | 54.02 | 43.87 |
| Mean (µg/m³) | 56.73 | 52.35 | 42.43 |
| Maximum (µg/m³) | 91.63 | 84.10 | 68.07 |

| Metric | S0 | S1 | S2 |
|---|---|---|---|
| Spatial standard deviation (μg/m³) | 16.86 | 15.80 | 12.05 |
| Points ≥75 μg/m³ | 2 | 2 | 0 |
| IDW exceedance area (m²) | 1.190 | 0.459 | 0 |

Table 4. Relative reductions between scenarios

| Comparison | Mean | Maximum | IDW exceedance area |
|---|---|---|---|
| S0 → S1 | 7.71% | 8.22% | 61.43% |
| S1 → S2 | 18.94% | 19.06% | 100% |
| S0 → S2 | 25.19% | 25.72% | 100% |

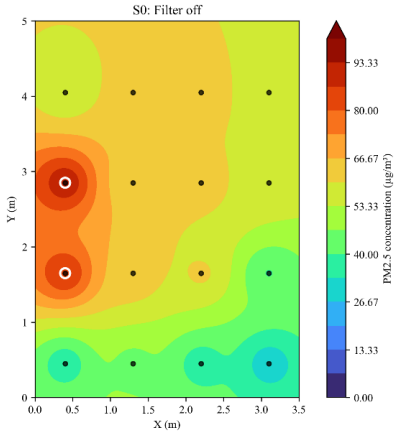



Figure 5. PM2.5 map for scenario S0

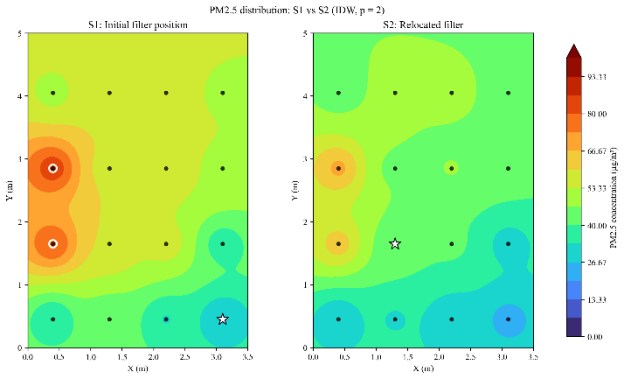



Figure 6. PM2.5 map for scenarios S1 and S2

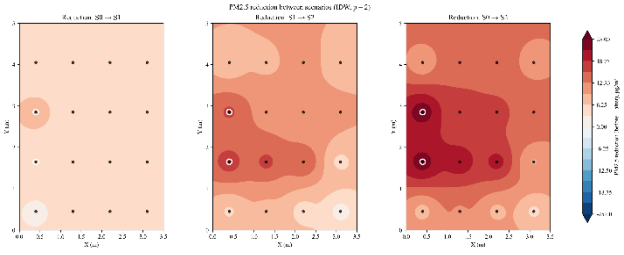


Figure 7. PM2.5 reduction between scenarios (IDW, p = 2)

### *3.2 Spatial interpretation of the scenario results*

The scenario comparison shows a consistent change in both central tendency and the upper end of the measured distribution. From S0 to S1, the mean decreased by 7.71% and the maximum decreased by 8.22%, while the IDW exceedance area decreased from 1.190 to 0.459 m². The two measured points above 75 μg/m³ remained in S1, so the initial purifier position reduced the overall level but did not remove the measured hotspot. After relocation in S2, the mean and maximum decreased by a further 18.94% and 19.06%, respectively, and no measured point exceeded the threshold. The spatial standard deviation also decreased from 16.86 in S0 to 12.05 μg/m³ in S2, indicating a less contrasting measured distribution under the tested conditions.

The result should not be interpreted as evidence that the purifier removed the same amount of PM2.5 from every part of the room. The IDW map estimates values between the measured points, and the estimated exceedance area changed more strongly than the point-based mean. This difference is expected because an interpolated boundary is sensitive to the positions of the sampling points and to the chosen exponent. The point measurements and the map therefore provide complementary information: the point values describe the recorded locations, while the IDW surface provides a visual estimate of the pattern between them.

### *3.3 Interpretation and limitations*

S2 had the lowest mean, maximum and mapped exceedance area among the three observed scenarios. The comparison is descriptive: sequential measurements cannot isolate the effect of relocating the purifier from changes in emissions or ventilation over time. The three block means at a location are not independent repeats. The sensor was not checked against a reference instrument, and optical PM readings can be affected by relative humidity and aerosol properties [3], [4].

The interpolated exceedance area also depends on the room boundary, grid resolution, sampling positions and IDW model. IDW does not model particle transport or airflow. Tests with a repeatedly randomized scenario order, logged activity and ventilation, a co-located reference monitor, and complete coordinate records would strengthen any placement claim. These room-scale observations should not be extrapolated to an industrial workshop without further validation.

### *3.4 Possible effect of purifier relocation*

S2 placed the purifier closer to the high-concentration region identified in the baseline map. The lower mean, maximum and mapped exceedance area suggest that this position performed better under the tested conditions. One possible explanation is that the purifier removed or mixed air from the source-adjacent area before it spread through the room. This explanation cannot be confirmed because air velocity, airflow direction, particle residence time and purifier CADR were not measured. The result should therefore be described as the best-performing tested configuration, not as the optimal location.

### *3.5 Comparison with recent studies*

The baseline results show that PM2.5 was not evenly distributed in the room. The S0 maximum of 91.63 μg/m³ was more than three times the minimum of 29.90 μg/m³, and the two measured hotspots were in the workstation area. This local difference is important because a room average may not represent the concentration near a possible source. Recent studies using distributed low-cost sensors also show that multiple measurement locations are useful for identifying local differences, but calibration and co-location are needed before these differences are interpreted quantitatively [7], [8].

The reductions observed after filtration are directionally consistent with field studies of portable air cleaners, but their magnitude should not be compared without considering the experimental setting. In the present study, the mean decreased by 7.71% from S0 to S1 and by a further 18.94% from S1 to S2. By contrast, a randomized crossover study in homes reported much larger reductions under a sustained filter condition, while a classroom study reported smaller absolute changes under low background concentrations [5], [12]. These differences are expected because removal depends on room volume, air-exchange rate, source strength, operating duration, filter setting, mixing and the location of the monitor relative to the cleaner. The present experiment is therefore most informative as a within-room placement comparison rather than as an estimate of universal purifier efficiency.

### *3.6 Implications for spatial monitoring*

The6 study also shows why spatial monitoring and filtration assessment should be considered together. If only one fixed point had been used, P09 could have suggested a much more severe condition than the storage-table area, while a point far from the workstation could have missed the hotspot. The IDW maps provide a simple way to show this difference and to identify possible locations for a purifier or a permanent monitor. However, the apparent hotspot boundary depends partly on the 16-point layout and the $p = 2$ weighting choice. Calibration studies emphasize the importance of co-location and environmental conditions [8], [9], [10]. For the mapping procedure used here, we recommend reporting these details together with the sampling coordinates and interpolation settings.

For a practical screening application, the results suggest that purifier placement should be considered together with the location of the likely source and the areas occupied by workers. A purifier placed away from the higher-concentration area may lower the room average while leaving a local hotspot. The present experiment supports this point only for the tested room and operating conditions. It does not show that the same placement will perform similarly in a larger room, a different ventilation arrangement or a workplace with a different source location.

### *3.7 Limitations and generalizability*

Several uncertainties limit generalization. First, the PMS5003 is an optical scattering sensor, so its response can vary with particle size, particle composition and relative humidity. Recent studies show that humidity-aware, environment-specific and machine-learning corrections can change the agreement between low-cost sensors and reference monitors [9], [11], [18], [19], [20], [21], [22], [23]. Second, sequential measurements can be affected by time trends. If emissions decreased naturally or a door remained closed for longer during S2, part of the improvement could be unrelated to relocation. Third, the IDW exceedance area is estimated from a model and is not a directly measured area. IDW also does not model particle transport or airflow. These issues do not

remove the observed difference between S0, S1 and S2, but the ranking should be checked with randomized repeats and independent validation.

### *3.8 Future validation protocol*

For a stronger validity assessment, a future experiment should include a co-location period with a reference-grade or well-characterized optical monitor. Temperature and relative humidity should be recorded at the same time. Calibration should then be evaluated using bias, mean absolute error, root mean square error and the coefficient of determination on data that were not used to fit the correction. Recent studies show that calibration performance depends on the duration of co-location and on the range of environmental conditions covered by the calibration data [7], [8], [9], [10]. For the placement experiment, the scenario order should also be randomized, purifier operating time should be standardized, and activity, doors, windows, fan state and source emissions should be logged.

### *3.9 Contribution and future work*

This study provides a simple method for screening PM2.5 distribution and comparing purifier positions in a laboratory room. It can help identify possible hotspots and generate ideas about purifier placement, but it is not yet suitable for regulatory compliance, occupational exposure certification or health-protection claims. The next experiment should repeat each scenario on multiple days, randomize the order, record temperature and relative humidity, include a reference monitor and report uncertainty for the scenario differences. It could also compare IDW with an airflow model and test whether the selected position remains effective when the source location changes.

## 4. CONCLUSIONS

This study used a portable ESP32-PMS5003 system to measure PM2.5 at 16 locations in a laboratory room and applied inverse distance weighting (IDW) to compare three air purifier configurations. The device validated UART frames and grouped 30 valid readings at each location into three consecutive block averages. The resulting maps were assessed using the mean and maximum concentrations, the number of measured hotspots, and the estimated hotspot area.

Among the three configurations, S2 produced the lowest measured concentrations. Compared with S1, mean PM2.5 decreased from 52.35 to 42.43 $\mu g/m^3$ (18.94%), while the maximum decreased from 84.10 to 68.07 $\mu g/m^3$ (19.06%). No measured point in S2 reached the study's hotspot threshold of 75 $\mu g/m^3$. These results identify S2 as the best of the configurations tested, but sequential measurements cannot establish that repositioning alone caused the observed reductions or that S2 is a globally optimal placement. Future work should compare the sensor with a reference instrument, collect simultaneous measurements at selected locations, and evaluate the method in an industrial workshop.

**Funding:** This research received no external funding.

**Conflicts of Interest:** The authors declare no conflict of interest.

**Publisher's Note:** All claims expressed in this article are solely those of the authors and do not necessarily represent those of their affiliated organizations, or those of the publisher, the editors and the reviewers.

## REFERENCES

[1] S. Masri, J. Rea, and J. Wu, "Use of low-cost sensors to characterize occupational exposure to PM2.5 concentrations inside an industrial facility in Santa Ana, CA: Results from a worker- and community-led pilot study," Atmosphere, vol. 13, no. 5, 2022, Art. no. 722, https://doi.org/10.3390/atmos13050722.

[2] R. Cao, B. Li, Z. Wang, Z.-R. Peng, S. Tao, and S. Lou, "Using a distributed air sensor network to investigate the spatiotemporal patterns of PM2.5 concentrations," Environ. Pollut., vol. 264, 2020, Art. no. 114549, https://doi.org/10.1016/j.envpol.2020.114549.

[3] R. Jayaratne, X. Liu, P. Thai, M. Dunbabin, and L. Morawska, "The influence of humidity on the performance of a low-cost air particle mass sensor and the effect of atmospheric fog," Atmos. Meas. Tech., vol. 11, no. 8, pp. 4883-4890, 2018, https://doi.org/10.5194/amt-11-4883-2018.

[4] A. Caseiro, S. Schmitz, and E. von Schneidemesser, "Particle number size distribution evaluation of Plantower PMS5003 low-cost PM sensors - A field experiment," Environ. Sci.: Atmos., vol. 4, no. 10, pp. 1183-1194, 2024, https://doi.org/10.1039/D4EA00086B.

[5] F. T. Lu et al., "Real-world effectiveness of portable air cleaners in reducing home particulate matter concentrations," Aerosol Air Qual. Res., vol. 24, no. 1, 2024, Art. no. 230202, https://doi.org/10.4209/aaqr.230202.

[6] D. Shepard, "A two-dimensional interpolation function for irregularly-spaced data," in Proc. 23rd ACM Nat. Conf., 1968, pp. 517-524, https://doi.org/10.1145/800186.810616.

[7] P. deSouza et al., "Calibrating networks of low-cost air quality sensors," Atmos. Meas. Tech., vol. 15, no. 21, pp. 6309-6328, 2022, https://doi.org/10.5194/amt-15-6309-2022.

[8] M. Levy Zamora, C. Buehler, A. Datta, D. R. Gentner, and K. Koehler, "Identifying optimal co-location calibration periods for low-cost sensors," Atmos. Meas. Tech., vol. 16, no. 1, pp. 169-179, 2023, https://doi.org/10.5194/amt-16-169-2023.

[9] M. Y. Patel, P. F. Vannucci, J. Kim, W. M. Berelson, and R. C. Cohen, "Towards a hygroscopic growth calibration for low-cost PM2.5 sensors," Atmos. Meas. Tech., vol. 17, no. 3, pp. 1051-1060, 2024, https://doi.org/10.5194/amt-17-1051-2024.

[10] M. Chacón-Mateos, H. García-Salamero, B. Laquai, and U. Vogt, "Calibration and performance evaluation of PM2.5 and NO2 air quality sensors for environmental epidemiology," Atmos. Meas. Tech., vol. 18, pp. 4061-4085, 2025, https://doi.org/10.5194/amt-18-4061-2025.

[11] G. Wang, C. Yu, K. Guo, H. Guo, and Y. Wang, "Research of low-cost air quality monitoring models with different machine learning algorithms," Atmos. Meas. Tech., vol. 17, no. 1, pp. 181-196, 2024, https://doi.org/10.5194/amt-17-181-2024.

[12] A. Azevedo, J. Liddie, J. Liu, J. E. Schiff, G. Adamkiewicz, and J. E. Hart, "Effects of portable air cleaners and A/C unit fans on classroom concentrations of particulate matter in a non-urban elementary school," PLOS ONE, vol. 17, no. 12, 2022, Art. no. e0278046, https://doi.org/10.1371/journal.pone.0278046.

[13] A. M. McIntyre et al., "Portable air cleaner usage and particulate matter exposure reduction in an environmental justice community: A pilot study," Environ. Health Insights, vol. 18, 2024, Art. no. 11786302241258587, https://doi.org/10.1177/11786302241258587.

[14] S. Sankhyan, J. K. Witteman, S. Coyan, S. Patel, and M. E. Vance, "Assessment of PM2.5 concentrations, transport, and mitigation in indoor environments using low-cost air quality monitors and a portable air cleaner," Environ. Sci.: Atmos., vol. 2, no. 4, pp. 647-658, 2022, https://doi.org/10.1039/D2EA00025C.

[15] Z. Sultan, J. Li, J. Pantelic, and S. Schiavon, "Indoor air pollution of outdoor origin: Mitigation using portable air cleaners in Singapore office building," Aerosol Air Qual. Res., vol. 22, no. 10, 2022, Art. no. 220204, https://doi.org/10.4209/aaqr.220204.

[16] Plantower, "*Digital universal particle concentration sensor: PMS5003 Series Data Manual,*" ver. 2.3, 2016. Accessed: Oct. 17, 2026. [Online]. Available: https://www.aqmd.gov/docs/default-source/aq-spec/resources-page/plantower-pms5003-manual_v2-3.pdf

[17] Espressif Systems, "*ESP32-WROOM-32D & ESP32-WROOM-32U Datasheet,*" 2026. Accessed: Oct. 17, 2026. [Online]. Available: https://www.espressif.com/sites/default/files/documentation/esp32-wroom-32d_esp32-wroom-32u_datasheet_en.pdf

[18] P. Gäbel and E. Hertig, "Recalibration of low-cost O3 and PM2.5 sensors: linking practices to recent air sensor test protocols," Atmos. Meas. Tech., vol. 19, no. 4, pp. 1293-1321, 2026, https://doi.org/10.5194/amt-19-1293-2026.

[19] J. Qian et al., "Enhancing accuracy of indoor air quality sensors via automated machine learning calibration," Atmos. Meas. Tech., vol. 19, no. 2, pp. 603-615, 2026, https://doi.org/10.5194/amt-19-603-2026.

[20] S. Mahajan and D. Helbing, "Dynamic calibration of low-cost PM2.5 sensors using trust-based consensus mechanisms," npj Clim. Atmos. Sci., vol. 8, no. 1, 2025, Art. no. 257, https://doi.org/10.1038/s41612-025-01145-2.

[21] L. Morawska, C. Asbach, and H. Patel, "Application of PM2.5 low-cost sensors for indoor air quality compliance monitoring," Aerosol Sci. Technol., vol. 59, no. 10, pp. 1210-1220, 2025, https://doi.org/10.1080/02786826.2025.2457326.

[22] S. Sousan, R. Wu, C. Popoviciu, S. Fresquez, and Y. M. Park, "Advancing low-cost air quality monitor calibration with machine learning methods," Environ. Pollut., vol. 374, 2025, Art. no. 126191, https://doi.org/10.1016/j.envpol.2025.126191.

[23] S. Koziel, A. Pietrenko-Dabrowska, M. Wojcikowski, and B. Pankiewicz, "Efficient field correction of low-cost particulate matter sensors using machine learning, mixed multiplicative/additive scaling and extended calibration inputs," Sci. Rep., vol. 15, no. 1, 2025, Art. no. 18573, https://doi.org/10.1038/s41598-025-02069-w.

[24] C. Zuidema et al., "Leveraging low-cost sensors to predict nitrogen dioxide for epidemiologic exposure assessment," J. Expo. Sci. Environ. Epidemiol., vol. 35, no. 2, pp. 169-179, 2025, https://doi.org/10.1038/s41370-024-00667-w.

## NOMENCLATURE

Table 5. Meaning of symbols used

| **Symbols** | **Meaning** |
|---|---|
| C(k) | k-th valid PM2.5 sample |
| R1-R3 | Average of three consecutive 10-sample blocks |
| $\overline{C}_i$ | Representative value at point i |
| $d_i$ | Distance from the interpolation location to point i |
| p | IDW exponent |
| Cavg, Cmax | Average and maximum concentrations |